

# Complexes of Platinum(II) Containing Neutral and Deprotonated 9-Methyladenine. Synthesis, X-ray Structures, and NMR Studies on the Cyclic Trimer $cis\text{-}[\text{L}_2\text{Pt}\{9\text{-MeAd}(-\text{H})\}]_3(\text{NO}_3)_3$ and the Dinuclear $cis\text{-}[\text{L}_2\text{Pt}(\text{ONO}_2)\{9\text{-MeAd}(-\text{H})\}\text{PtL}_2](\text{NO}_3)_2$ (L = PMePh<sub>2</sub>)

Bruno Longato,<sup>\*,†,‡</sup> Lucia Pasquato,<sup>‡</sup> Adele Mucci,<sup>§</sup> Luisa Schenetti,<sup>§</sup> and Ennio Zangrando<sup>||</sup>

Istituto di Scienze e Tecnologie Molecolari—CNR, c/o Dipartimento di Chimica Inorganica, Metallorganica ed Analitica, Università di Padova, Via Marzolo 1, 35131 Padova, Italy, Dipartimento di Chimica Inorganica, Metallorganica ed Analitica, Università di Padova, Via Marzolo 1, 35131 Padova, Italy, Dipartimento di Chimica, Università di Modena e Reggio Emilia, Via Campi 183, 41100 Modena, Italy, and Dipartimento di Scienze Chimiche, Università di Trieste, Via Giorgieri 1, 34127 Trieste, Italy

Received April 17, 2003

The dinuclear hydroxo complex  $cis\text{-}[\text{L}_2\text{Pt}(\mu\text{-OH})_2(\text{NO}_3)_2]$  (L = PMePh<sub>2</sub>, **1**), in CH<sub>2</sub>Cl<sub>2</sub>, CH<sub>3</sub>CN, or DMF solution, deprotonates the NH<sub>2</sub> group of 9-methyladenine (9-MeAd) to give the complex  $cis\text{-}[\text{L}_2\text{Pt}\{9\text{-MeAd}(-\text{H})\}]_3(\text{NO}_3)_3$ , **2**, which was isolated in good yield. The X-ray structure shows that the nucleobase binds symmetrically the metal centers through the N(1),N(6) atoms forming a cyclic trimer with Pt···Pt distances in the range 5.202(1)–5.382(1) Å. Dissolution of **2** in DMSO or DMF determines the partial (or total) dissociation of the cyclic structure to form several fragments. A multinuclear NMR analysis of the resulting mixture supports the presence of the mononuclear species  $cis\text{-}[\text{L}_2\text{Pt}\{9\text{-MeAd}(-\text{H})\}]^+$ , **3**, in which the deprotonated nucleobase chelates the metal center with the N(6),N(7) atoms. Addition of a stoichiometric amount of the nitrate complex  $cis\text{-}[\text{L}_2\text{Pt}(\text{ONO}_2)_2]$  (L = PMePh<sub>2</sub>, **4**) to a DMSO or DMF solution of **2** affords quantitatively the diplatinated compound  $cis\text{-}[\text{L}_2\text{Pt}(\text{ONO}_2)\{9\text{-MeAd}(-\text{H})\}\text{PtL}_2](\text{NO}_3)_2$ , **5**. The single-crystal X-ray analysis shows that the adenine behaves as a tridentate ligand bridging two  $cis\text{-L}_2\text{Pt}$  units at the N(1) and N(6),N(7) sites, respectively [Pt(1)–N(1) = 2.109(5) Å, Pt(2)–N(6) = 2.095(7) Å, Pt(2)–N(7) = 2.126(7) Å]. The N(1)-bonded metal center completes the coordination sphere through an oxygen atom of a nitrate group, and its coordination plane is arranged orthogonally with respect the second one. The Pt–O distance [2.109(5) Å] is similar to those found in the nitrate complex **4** [2.110 Å, average]. The related complex  $cis\text{-}[\text{L}_2\text{Pt}(\text{ONO}_2)_2(9\text{-MeAd})](\text{NO}_3)_2$ , **6**, containing the neutral adenine platinated at the N(1),N(7) atoms, was isolated and its stability in solution investigated by NMR spectroscopy. In DMSO, **6** undergoes decomposition forming a mixture of the species **4**, **5**, and the adenine mono- and bis-adducts  $cis\text{-}[\text{L}_2\text{Pt}(9\text{-MeAd})(\text{DMSO})]^{2+}$ , **7**, and  $cis\text{-}[\text{L}_2\text{Pt}(9\text{-MeAd})_2]^{2+}$ , **8**, respectively. This last complex, quantitatively formed upon addition of 9-MeAd (Pt/adenine = 1:2) to the mixture, was also isolated and characterized.

## Introduction

Since the discovery of the biological activity of *cisplatin*, a large part of the coordination chemistry of DNA compo-

nents toward the platinum has been carried out on complexes of Pt<sup>II</sup> (and Pt<sup>IV</sup>) having NH<sub>3</sub> or amines as ancillary ligands.<sup>1,2</sup> In the frame of our interest in the reactivity of the *cisplatin* analogues  $cis\text{-}[\text{L}_2\text{PtCl}_2]$  (L = phosphorus donor atom of a tertiary phosphine) with model nucleobases, we described the binding modes of 9-substituted methyladenine (9-MeAd) in the neutral and cationic complexes  $cis\text{-}[(\text{PMe}_3)_2\text{Pt}(\text{ONO}_2)_2]$

\* To whom correspondence should be addressed. E-mail: longato@chin.unipd.it.

† Istituto di Scienze e Tecnologie Molecolari—CNR, c/o Dipartimento di Chimica Inorganica, Metallorganica ed Analitica, Università di Padova.

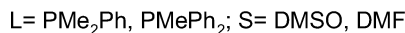
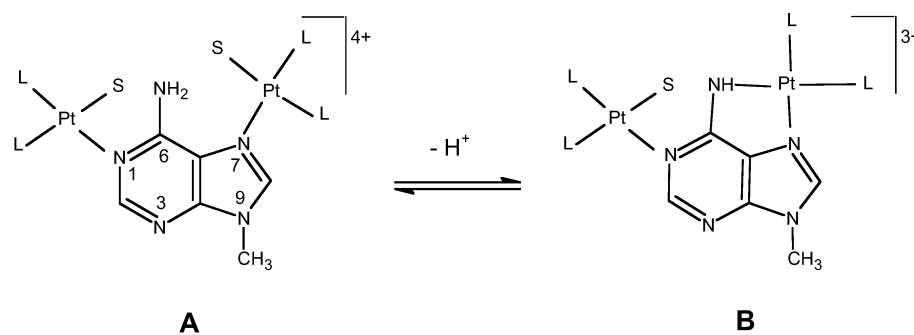
‡ Dipartimento di Chimica Inorganica, Metallorganica ed Analitica, Università di Padova.

§ Università di Modena e Reggio Emilia.

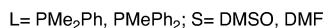
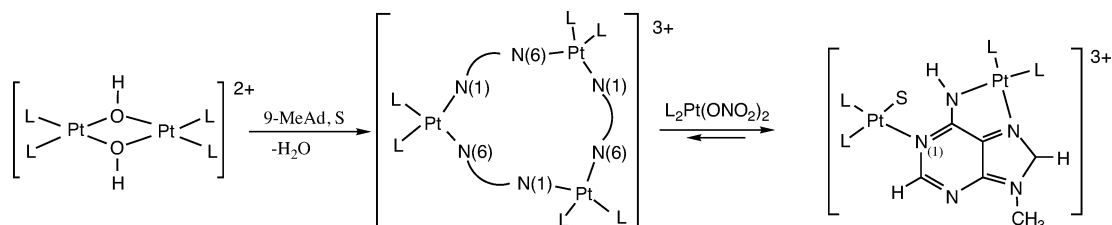
|| Università di Trieste.

(1) Lippert, B. *Prog. Inorg. Chem.* **1989**, *37*, 1–97 and references therein.  
(2) Lippert, B. *Coord. Chem. Rev.* **2000**, *200–202*, 487–516.

Scheme 1



Scheme 2



and  $\text{cis}-[(\text{PMe}_3)_2\text{Pt}(\mu\text{-OH})_2]^{2+}$ , respectively.<sup>3</sup> In the first case the substitution of the nitrate ligands afforded the bis-adduct  $\text{cis}-[(\text{PMe}_3)_2\text{Pt}(9\text{-MeAd})_2]^{2+}$ , in which the neutral adenines are selectively platinated at the N(1) site, while the cationic hydroxo complex deprotonated the exocyclic amino group to form  $\text{cis}-[(\text{PMe}_3)_2\text{Pt}\{9\text{-MeAd}(-\text{H})\}]_2^{2+}$ . The X-ray characterization of this dinuclear compound, carried out on the 9-ethyl-substituted adenine, disclosed a cyclic structure in which the nucleobase acts as bridging ligand through the N(1),N(6) atoms.

More recently, a detailed NMR study on the reaction of  $\text{cis}-[(\text{PMe}_2\text{Ph})_2\text{Pt}(\text{ONO}_2)_2]$  with variable amounts of nucleobase in DMSO- $d_6$  allowed us to characterize a diplatinated complex (species **B** in Scheme 1) resulting on the simultaneous binding of two  $\text{cis}-\{(\text{PMe}_2\text{Ph})_2\text{Pt}\}$  units at the N(1) and N(7) atoms of the adenine with concomitant reversible deprotonation of the exocyclic  $\text{NH}_2$  group. By increasing the Pt/adenine ratio to the value 1:2, in fact, the complete disappearance of the chelated complex **B** was observed with the almost quantitative formation of the bis-adduct  $\text{cis}-[(\text{PMe}_2\text{Ph})_2\text{Pt}(9\text{-MeAd})_2]^{2+}$  in which the selectivity of the metal center toward the N(1) site of the adenine was maintained.<sup>5</sup>

The complete spectroscopic characterization of **B** was possible by taking advantage of the observation that this complex was formed when the trinuclear species  $\text{cis}-[(\text{PMe}_2\text{Ph})_2\text{Pt}\{9\text{-MeAd}(-\text{H})\}]_3^{3+}$ , obtained by reacting  $\text{cis}-[(\text{PMe}_2\text{Ph})_2\text{Pt}(\mu\text{-OH})_2](\text{NO}_3)_2$  with 9-MeAd, was treated with  $\text{cis}-[(\text{PMe}_2\text{Ph})_2\text{Pt}(\text{ONO}_2)_2]$ , according to the reaction scheme depicted in Scheme 2.

Now, the extension of this study to the complexes stabilized by the less basic but more sterically demanding  $\text{PMePh}_2$  (L) ligand, i.e.,  $\text{cis}-[\text{L}_2\text{Pt}(\mu\text{-OH})_2](\text{NO}_3)_2$ , **1**, and  $\text{cis}-[\text{L}_2\text{Pt}(\text{ONO}_2)_2]$ , **4**, has permitted the determination of the crystal structures of  $\text{cis}-[\text{L}_2\text{Pt}\{9\text{-MeAd}(-\text{H})\}]_3(\text{NO}_3)_3$  (**2**) and  $\text{cis}-[\text{L}_2\text{Pt}(\text{ONO}_2)_2\{9\text{-MeAd}(-\text{H})\}\text{PtL}_2](\text{NO}_3)_2$  (**5**), both described in this paper. Complex **2** and its  $\text{PMe}_2\text{Ph}$  analogue represent the first examples of cyclic trimers of the N(1),N(6)-platinated adenine ion, whereas the binding mode of the adenine found in **5** (species **B** in Scheme 1) has been only recently proved for a platinum(IV) organometallic compound.<sup>6</sup> The new compounds have been characterized by multinuclear NMR spectroscopy showing that **2** in coordinating solvents is in equilibrium with the mononuclear species  $\text{cis}-[\text{L}_2\text{Pt}\{9\text{-MeAd}(-\text{H})\}]^+$  (**3**) in which the nucleobase chelates the metal center with the N(6),N(7) atoms. In addition, in this paper we describe the synthesis of  $\text{cis}-[\{\text{L}_2\text{Pt}(\text{ONO}_2)_2\}_2(9\text{-MeAd})](\text{NO}_3)_2$ , (**6**), containing the neutral adenine bridging two metal centers through the N(1) and N(7) atoms. The spectroscopic characterization (<sup>31</sup>P NMR) reveals that **6**, in DMSO, forms a mixture of the species **4**, **5**, and  $\text{cis}-[\text{L}_2\text{Pt}(9\text{-MeAd})(\text{DMSO})]^{2+}$ , **7**, which are quantitatively converted into the bis-adduct  $\text{cis}-[\text{L}_2\text{Pt}(9\text{-MeAd})_2](\text{NO}_3)_2$  (**8**) upon addition of a stoichiometric amount of

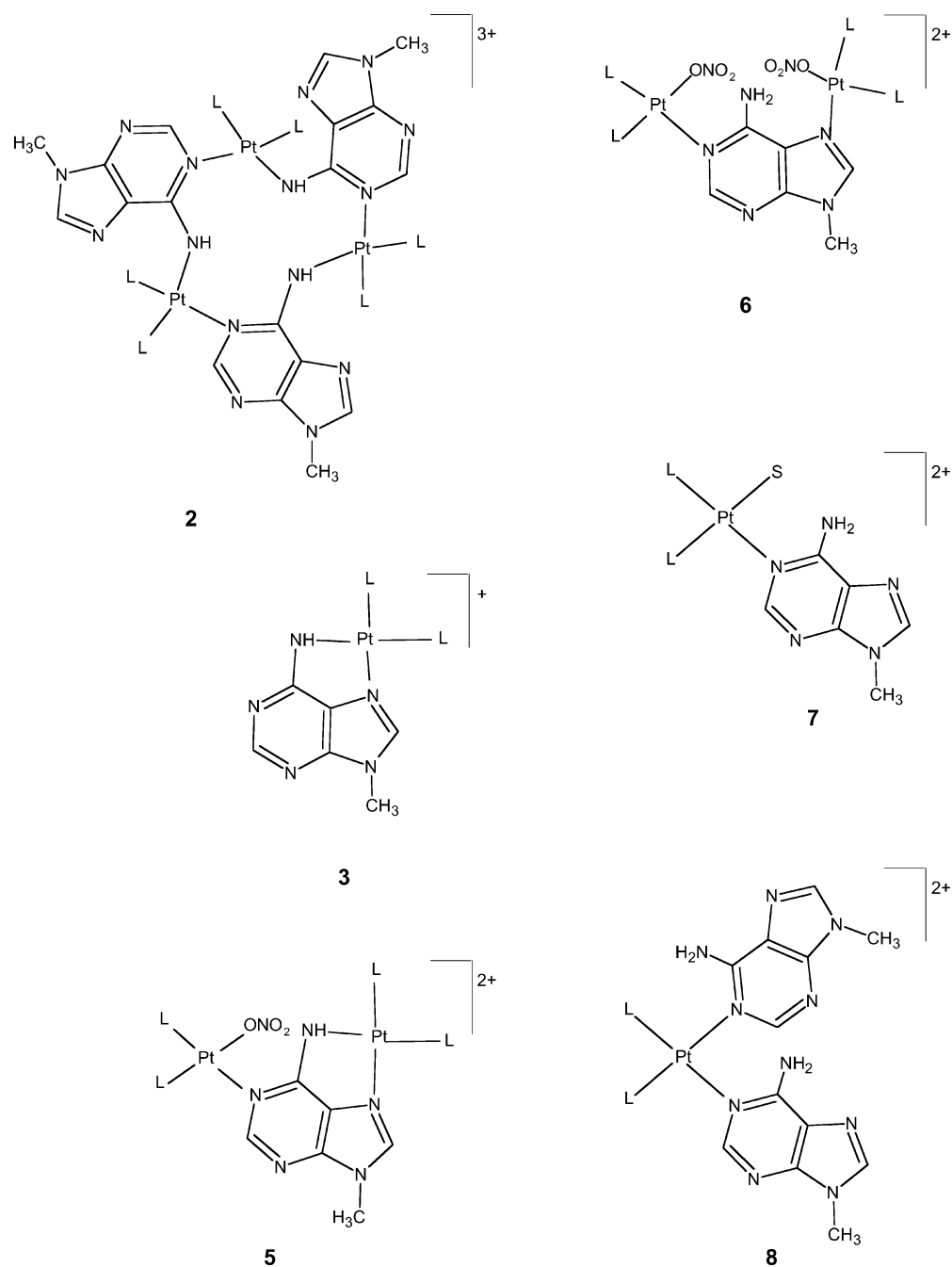
(3) Schenetti, L.; Mucci, A.; Longato, B. *J. Chem. Soc., Dalton Trans.* **1996**, 299–303.

(4) Trovò, G.; Bandoli, G.; Nicolini, M.; Longato, B. *Inorg. Chim. Acta* **1993**, *211*, 95–99.

(5) Longato, B.; Pasquato, L.; Mucci, A.; Schenetti, L. *Eur. J. Inorg. Chem.* **2003**, 128–137.

(6) Zhu, X.; Rusanov, E.; Kluge, R.; Schmidt, H.; Steinborn, D. *Inorg. Chem.* **2002**, *41*, 2667–2671.

Chart 1



9-MeAd. A graphical scheme of all the characterized adenine complexes is presented in Chart 1.

### Experimental Section

**Instrumentation and Materials.** <sup>1</sup>H, <sup>13</sup>C, <sup>15</sup>N, <sup>31</sup>P, and <sup>195</sup>Pt NMR spectra were obtained with a Bruker 400 AMX WB and a Bruker AVANCE 300. Reagent grade chemicals were used as received unless otherwise stated. *cis*-[(PMePh<sub>2</sub>)<sub>2</sub>PtCl<sub>2</sub>]<sup>7</sup> and 9-MeAd<sup>8</sup> were prepared according to the literature methods. *cis*-[L<sub>2</sub>Pt(μ-

OH)]<sub>2</sub>(NO<sub>3</sub>)<sub>2</sub> (L = PMePh<sub>2</sub>, **1**)<sup>9</sup> was synthesized with a procedure similar to that described for the PMe<sub>2</sub>Ph analogue.<sup>3</sup>

**Synthetic Work.** *cis*-[(PMePh<sub>2</sub>)<sub>2</sub>Pt{9-MeAd(-H)}]<sub>3</sub>(NO<sub>3</sub>)<sub>3</sub> (**2**). A suspension of **1**, *cis*-[(PMePh<sub>2</sub>)<sub>2</sub>Pt(μ-OH)]<sub>2</sub>(NO<sub>3</sub>)<sub>2</sub> (150 mg, 0.11 mmol), and 9-MeAd (33 mg, 0.22 mmol) in CH<sub>3</sub>CN (2.5 mL) was stirred at room temperature for ca. 20 min. The addition of Et<sub>2</sub>O to the resulting solution afforded a white microcrystalline solid, which was filtered and dried under vacuum. The isolated product weighed 140 mg (yield 78%, calculated as anhydrous product). The crystals used for the X-ray analysis, obtained by slow evaporation of a dichloromethane/toluene (1:1) solution of **2** at ambient conditions,

(7) Jenkins, J. M.; Shaw, L. *J. Chem. Soc. A* **1966**, 773–775.

(8) Talman, E. G.; Brüning, W.; Reedijk, J.; Spek, A. L.; Veldman, N. *Inorg. Chem.* **1997**, *36*, 854–861.

(9) Longato, B.; Dolmella, A.; Bandoli, G. *Eur. J. Inorg. Chem.*, submitted.

had the composition  $2 \cdot 0.75\text{H}_2\text{O}$  whereas the elemental analysis was more consistent with the formulation  $2 \cdot 3\text{H}_2\text{O}$ . Anal. Calcd for  $\text{C}_{32}\text{H}_{32}\text{N}_6\text{O}_3\text{P}_2\text{Pt} \cdot \text{H}_2\text{O}$ : C, 46.66; H, 4.16; N, 10.20. Found: C, 46.84; H, 4.02; N, 9.95.  $^{31}\text{P}$  NMR (121.5 MHz, in  $\text{CD}_3\text{CN}$ ):  $\delta$  -8.50 ( $^1J_{\text{PPt}}$  3192 Hz), -9.34 ( $^1J_{\text{PPt}}$  3372 Hz) with  $^2J_{\text{PP}}$  23.3 Hz.  $^1\text{H}$  NMR (400.13 MHz, in  $\text{CDCl}_3$ ):  $\delta$  major component (ca. 90%) 8.27 (s, 1H, H(8)), 7.65 (s, 1H, H(2)), 8.2–6.4 (m, 20 H, Ph), 7.11 (br s, 1H, NH), 3.45 (s, 3H, NMe), 2.75 (d,  $^2J_{\text{HP}}$  11.4 Hz, 3H, PMe), 1.20 (d,  $^2J_{\text{HP}}$  10.3 Hz, 3H, PMe); minor component 8.14 (s, 1H, H(2)), 6.82 (s, 1H, H(8)), 8.2–6.4 (m, 20 H, Ph), 5.8 (br s, 1H, NH), 3.73 (s, 3 H, NMe), 2.33 (d,  $^2J_{\text{HP}}$  10 Hz, 3H, PMe), 1.83 (d,  $^2J_{\text{HP}}$  10 Hz, 3H, PMe).  $^{13}\text{C}$  NMR (100.61 MHz, in  $\text{CDCl}_3$ ):  $\delta$  166.2 (C-6), 155.8 (C-2), 154.5 (C-4), 141.8 (C-8), 128.3 (C-5), 30.2 (NCH<sub>3</sub>), 16.2 and 13.3 (PCH<sub>3</sub>).

$^1\text{H}$  NMR (400.13 MHz, in  $\text{DMSO}-d_6$ ):  $\delta$  major component (ca. 60%) 8.04 (s, 1H, H(8)), 6.52 (s, 1H, H(2)), 5.25 (br s, 1H, NH), 3.56 (s, 3H, NMe), 2.23 (d,  $^2J_{\text{HP}}$  10 Hz, 3H, PMe), 2.12 (d,  $^2J_{\text{HP}}$  10 Hz, 3H, PMe).  $^{13}\text{C}$  NMR (100.61 MHz, in  $\text{DMSO}-d_6$ ):  $\delta$  164.9 (C-6), 157.8 (C-2), 147.5 (C-4), 140.1 (C-8), 128.3 (C-5), 30.6 (NCH<sub>3</sub>), 13.2 and 12.1 (PCH<sub>3</sub>).

With the same procedure, complex **2** was obtained operating in  $\text{CH}_2\text{Cl}_2$  (isolated product 276 mg, yield 77%) and DMF (160 mg, yield 88%).

**cis-[(PMePh<sub>2</sub>)<sub>2</sub>Pt(ONO<sub>2</sub>)<sub>2</sub>] (4)**. A solution of  $\text{AgNO}_3$  (0.52 g, 3.06 mmol) in EtOH (8 mL) and  $\text{H}_2\text{O}$  (1.5 mL) was slowly added to a  $\text{CH}_2\text{Cl}_2$  (13 mL) solution of **cis-[(PMePh<sub>2</sub>)<sub>2</sub>PtCl<sub>2</sub>]** (1.02 g, 1.53 mmol). The resulting precipitate was eliminated by filtration and the solvent evaporated to dryness under vacuum, yielding 1.05 g of product (yield 95%). The isolated solid contained small amounts of  $\text{CH}_2\text{Cl}_2$ , seen by  $^1\text{H}$  NMR. Anal. Calcd for  $\text{C}_{26}\text{H}_{26}\text{N}_2\text{O}_6\text{P}_2\text{Pt} \cdot 0.5\text{CH}_2\text{Cl}_2$ : C, 41.77; H, 3.57; N, 3.68. Found: C, 41.72; H, 3.42; N, 3.44.  $^1\text{H}$  NMR (300 MHz, in  $\text{DMSO}-d_6$ ):  $\delta$  7.64–7.43 (m, 20H, Ph), 2.02 (d,  $^2J_{\text{HP}}$  10.6 Hz, 6H, PMe).  $^{31}\text{P}$  NMR (121.5 MHz, in  $\text{DMSO}-d_6$ ):  $\delta$  -6.90 (s,  $^1J_{\text{PPt}}$  3903 Hz).

**cis-[(PMePh<sub>2</sub>)<sub>2</sub>Pt(ONO<sub>2</sub>)<sub>2</sub>{9-MeAd(-H)}Pt(PMePh<sub>2</sub>)<sub>2</sub>](NO<sub>3</sub>)<sub>2</sub> (5)**. To a solution of **2** (135 mg, 0.056 mmol) in DMF (5 mL) was added **4** (121 mg, 0.168 mmol), and the resulting solution was stirred at room temperature for 2 h. Addition of  $\text{Et}_2\text{O}$  gave a white solid, which was filtered, washed with  $\text{Et}_2\text{O}$ , and dried under vacuum. Crystallization of the crude product, by dissolution in DMF and vapor diffusion of  $\text{Et}_2\text{O}$ , afforded X-ray quality crystals of **5** (192 mg, yield 68%) having the formula **cis-[(PMePh<sub>2</sub>)<sub>2</sub>Pt(ONO<sub>2</sub>)<sub>2</sub>{9-MeAd(-H)}Pt(PMePh<sub>2</sub>)<sub>2</sub>](NO<sub>3</sub>)<sub>2</sub>·2DMF (5·2DMF)**. Anal. Calcd for  $\text{C}_{64}\text{H}_{72}\text{N}_{10}\text{O}_{11}\text{P}_4\text{Pt}_2$  (1671.4): C, 45.99; H, 4.34; N, 8.38. Found: C, 45.69; H, 4.35; N, 8.64.  $^1\text{H}$  NMR (400.13, in  $\text{DMSO}-d_6$ ):  $\delta$  8.64 (s, 1H, H(2)), 7.8–7.2 (m, 40 H, Ph), 6.52 (s, 1H, H(8)), 5.30 (br s, 1H, NH), 3.56 (s, 3H, NMe), 2.50 (s, 6H, PMe), 2.26 (d,  $^2J_{\text{HP}}$  11.1 Hz, 3H, PMe), 1.97 (d,  $^2J_{\text{HP}}$  11.1 Hz, 3H, PMe); DMF resonances at 7.9(s), 2.89 (s), and 2.73 (s).  $^{13}\text{C}$  NMR (100.6 MHz, in  $\text{DMSO}-d_6$ ):  $\delta$  164.9 (C-6), 157.8 (C-2), 147.5 (C-4), 140.1 (C-8), 124.9 (C-5), 30.6 (NCH<sub>3</sub>), 13.2 and 12.1 (PCH<sub>3</sub>).

**cis-[(PMePh<sub>2</sub>)<sub>2</sub>Pt(ONO<sub>2</sub>)<sub>2</sub>]{9-MeAd}(NO<sub>3</sub>)<sub>2</sub> (6)**. 9-MeAd (18.8 mg, 0.13 mmol) was added to a suspension of **4** (182 mg, 0.25 mmol) in  $\text{CHCl}_3$  (8 mL) and stirred at ambient temperature for 1 h. Addition of  $\text{Et}_2\text{O}$  to the resulting solution afforded a white solid, which was recovered by filtration, washed several times with  $\text{Et}_2\text{O}$ , and dried under vacuum. The yield of **6** was 160 mg (80%). Anal. Calcd for  $\text{C}_{58}\text{H}_{59}\text{N}_9\text{O}_{12}\text{P}_4\text{Pt}_2$  (1588.2): C, 43.86; H, 3.74; N, 7.94. Found: C, 43.35; H, 3.44; N, 7.87.  $^1\text{H}$  NMR (400.13, in  $\text{CDCl}_3$ )  $\delta$ : 11.08 (br s, 1H, NH<sub>2</sub>), 9.94 (s, 1H, H(8)), 8.53 (br s, 1H, NH<sub>2</sub>), 8.01 (s, 1H, H(2)), 8.0–6.9 (m, 40 H, Ph), 3.52 (s, 3H, NMe), 2.39 (d,  $^2J_{\text{HP}}$  11.6 Hz, 3H, PMe), 2.26 (d,  $^2J_{\text{HP}}$  11.3 Hz, 3H, PMe), 2.13 (d,  $^2J_{\text{HP}}$  11.3 Hz, 3H, PMe), 1.96 (d,  $^2J_{\text{HP}}$  11.4 Hz, 3H, PMe).

**Table 1.** Crystallographic Data and Details of Structural Refinement Parameters for **2**, **4**, and **5**

	2·0.75H <sub>2</sub> O	4·0.5CH <sub>2</sub> Cl <sub>2</sub>	5·2DMF
formula	C <sub>96</sub> H <sub>97.5</sub> N <sub>18</sub> -O <sub>9.75</sub> P <sub>6</sub> Pt <sub>3</sub>	C <sub>26.50</sub> H <sub>27</sub> CIN <sub>2</sub> -O <sub>6</sub> P <sub>2</sub> Pt	C <sub>64</sub> H <sub>72</sub> N <sub>10</sub> -O <sub>11</sub> P <sub>4</sub> Pt <sub>2</sub>
fw	2430.51	761.98	1671.38
crystal system	monoclinic	monoclinic	triclinic
space group	P2 <sub>1</sub> /n	P2 <sub>1</sub> /c	P1
a, Å	30.144(6)	10.947(3)	13.805(4)
b, Å	18.216(4)	13.230(4)	14.515(4)
c, Å	36.300(6)	21.344(5)	20.672(5)
α, deg			76.72(2)
β, deg	93.58(4)	90.11(2)	75.59(3)
γ, deg			65.96(3)
V, Å <sup>3</sup>	19893(7)	3091.2(15)	3625.1(17)
Z	8	4	2
D <sub>calcd</sub> , g cm <sup>-3</sup>	1.623	1.637	1.531
μ, mm <sup>-1</sup>	7.003	4.769	4.004
F(000)	9612	1492	1660
θ range, deg	2.50–33.13	2.45–27.10	1.79–27.88
reflns collected	47103	11190	28765
reflns unique	25026	6149	15805
reflns I > 2σ(I)	20185	4654	10820
no. of params	1285	346	800
R(int)	0.0549	0.0507	0.0519
GOF on F <sup>2</sup>	1.021	1.053	1.054
R1 <sup>a</sup>	0.0746	0.0492	0.0553
wR2 <sup>a</sup>	0.2081	0.1424	0.1578
residuals, e·Å <sup>-3</sup>	2.154, -1.191	1.085, -0.888	1.300, -2.576

$$^a R1 = \sum |F_o| - |F_c| / \sum |F_o|, wR2 = [\sum w(F_o^2 - F_c^2)^2 / \sum w(F_o^2)^2]^{1/2}.$$

$^{13}\text{C}$  NMR (100.61 MHz, in  $\text{CDCl}_3$ ):  $\delta$  153.3 (C-2), 152.2 (C-6), 147.8 (C-8), 146.6 (C-4), 115.5 (C-5), 30.9 (NCH<sub>3</sub>), 13.1, 12.4, and 9.5 (PCH<sub>3</sub>).

**cis-[(PMePh<sub>2</sub>)<sub>2</sub>Pt(9-MeAd)<sub>2</sub>](NO<sub>3</sub>)<sub>2</sub> (8)**. 9-MeAd (57 mg, 0.4 mmol) was added to a solution of **4** (137 mg, 0.2 mmol) in  $\text{CH}_3\text{CN}$  (7 mL) and stirred for 1 h. The resulting solution, left at ambient temperature for 5 days, separated a white solid, which was recovered by filtration, washed with  $\text{Et}_2\text{O}$ , and dried under vacuum. The yield of **8** was 170 mg (88%). Anal. Calcd for  $\text{C}_{38}\text{H}_{40}\text{N}_{12}\text{O}_6\text{P}_2\text{Pt}$ : C, 44.84; H, 3.96; N, 16.51. Found: C, 44.71; H, 3.92; N, 16.46. The solid, insoluble in chlorinated solvents, was characterized in  $\text{DMSO}$ .  $^1\text{H}$  NMR (400.13, in  $\text{DMSO}-d_6$ ):  $\delta$  major conformer (ca. 55%) 8.95 (s, 2H, H(2)), 8.6 (br s, 4H, NH<sub>2</sub>), 8.12 (s, 2H, H(8)), 7.7–6.8 (m, 20 H, Ph), 3.60 (s, 6H, NMe), 2.32 (d,  $^2J_{\text{HP}}$  11 Hz, 6H, PMe); minor conformer (45%) 8.71 (s, 2H, H(2)), 8.6 (br s, 4H, NH<sub>2</sub>), 8.11 (s, 2H, H(8)), 7.7–6.8 (m, 20 H, Ph), 3.57 (s, 6H, NMe), 2.32 (d,  $^2J_{\text{HP}}$  11 Hz, 6H, PMe).  $^{13}\text{C}$  NMR (100.61 MHz, in  $\text{DMSO}-d_6$ ):  $\delta$  more abundant conformer 155.0 (C-6), 152.1 (C-2), 148.8 (C-4), 144.8 (C-8), 120.5 (C-5), 29.6 (NCH<sub>3</sub>), 10.8 (PCH<sub>3</sub>); less abundant conformer 154.4 (C-6), 153.1 (C-2), 148.7 (C-4), 144.8 (C-8), 120.7 (C-5), 29.6 (NCH<sub>3</sub>), 10.8 (PCH<sub>3</sub>).

**X-ray Structure Determinations.** Crystal data, data collection, and refinement parameters for compounds **2**, **4**, and **5** are summarized in Table 1. Due to the small crystal dimensions (approximately  $0.15 \times 0.14 \times 0.10$  mm), data collection of **2** was carried out at the X-ray diffraction beamline of the Synchrotron Elettra, Trieste, Italy, using a monochromatized wavelength of 1.000 Å. A total of 60 frames were collected on a 165 mm CCD MarResearch (rotation of 3° about  $\varphi$ , fixed dose of radiation, detector at 35 mm from the crystal,  $T = 100(2)$  K). Data collections of **4** and **5** were performed on a Nonius DIP-1030H system equipped with Mo-K $\alpha$  radiation ( $\lambda = 0.71073$  Å) graphite-monochromatized (30 frames, exposure time of 20 min, rotation of 6° about  $\varphi$ , detector at 80 mm from the crystal,  $T = 293(2)$  K). Cell refinement, indexing, and scaling of all the data sets were



## Pt(II) Complexes Containing 9-Methyladenine

performed using programs Mosflm and Scala.<sup>10</sup> The structures were solved by Patterson and subsequent Fourier analyses and refined by the full-matrix least-squares method based on  $F^2$  with all observed reflections.<sup>11</sup> In **2** all the phenyl rings were fitted to regular hexagons and isotropically refined; four disordered nitrate anions with restrained geometry were treated isotropically (fixed  $U = 0.25$ ); three residuals were interpreted as water molecules with half-occupancy. A difference Fourier map revealed the presence of a disordered  $\text{CH}_2\text{Cl}_2$  molecule (0.5 occupancy) in **4** and of two DMF molecules in **5**. The contributions of hydrogen atoms at calculated positions were included in final cycles of refinements. All the calculations were performed using the WinGX System, version 1.64.<sup>12</sup>

## Results and Discussion

**Synthesis and Structure of the Trinuclear Complex  $cis\text{-}[(\text{PMePh}_2)_2\text{Pt}\{9\text{-MeAd}(-\text{H})\}]_3(\text{NO}_3)_3$ , **2**.** We have already shown that the dinuclear hydroxo complexes  $cis\text{-}[\text{L}_2\text{Pt}(\mu\text{-OH})]_2^{2+}$  in DMSO deprotonate the exocyclic amino group of the 9-substituted methyladenine to form the dinuclear complex  $cis\text{-}[\text{L}_2\text{Pt}\{9\text{-MeAd}(-\text{H})\}]_2^{2+}$  when L is  $\text{PMe}_3$ <sup>3</sup> or the trinuclear species  $cis\text{-}[\text{L}_2\text{Pt}\{9\text{-MeAd}(-\text{H})\}]_3^{3+}$  when L is  $\text{PMe}_2\text{Ph}$ .<sup>5</sup> Both are cyclic compounds in which the nucleobases act as bridging ligands binding two  $cis\text{-L}_2\text{Pt}$  units through the N(1),N(6) atoms.

The hydroxo complex, **1**, stabilized by the bulkier phosphine  $\text{PMePh}_2$ , is also very reactive toward this model nucleobase. <sup>31</sup>P NMR experiments carried out in  $\text{DMSO-}d_6$  show a rapid and complete disappearance of the signals typical of **1** when the stoichiometric amount of 9-MeAd is added. In this case, however, the multiplicity of resonances observed indicates the formation of a complex mixture of products. On the contrary, in acetonitrile or chlorinated solvents, the spectra of the resulting solutions show signals due to the predominant species  $cis\text{-}[(\text{PMePh}_2)_2\text{Pt}\{9\text{-MeAd}(-\text{H})\}]_3^{3+}$ , **2**, which has been isolated in fairly good yields. Crystallization of the product from a mixture of  $\text{CH}_2\text{Cl}_2$ /toluene afforded small but well-shaped crystals, suitable for an X-ray diffraction study, having the composition  $cis\text{-}[(\text{PMePh}_2)_2\text{Pt}\{9\text{-MeAd}(-\text{H})\}]_3(\text{NO}_3)_3 \cdot 0.75\text{H}_2\text{O}$  (**2**·0.75H<sub>2</sub>O). The X-ray analysis confirms for **2** the trinuclear arrangement with a pseudo-3-fold symmetry. Two crystallographically independent complexes, but with a close comparable conformation, were found in the unit cell. As depicted in Figure 1, the deprotonated 9-methyladenine acts as a bridging ligand through N(1) and N(6) donors toward the platinum centers. The Pt–N(6) mean bond lengths are fairly shorter when compared with those involving N(1) (mean values of 2.075(10) and 2.117(10) Å, respectively), although the low accuracy on bond distances does not allow a detailed analysis. The Pt–P bond distances average to 2.280(4) Å. The intermetallic distances vary from 5.202(1) Å, and one of these (ca. 5.20 Å) is significantly shorter with respect to the other two (mean 5.36 Å) in both the complexes

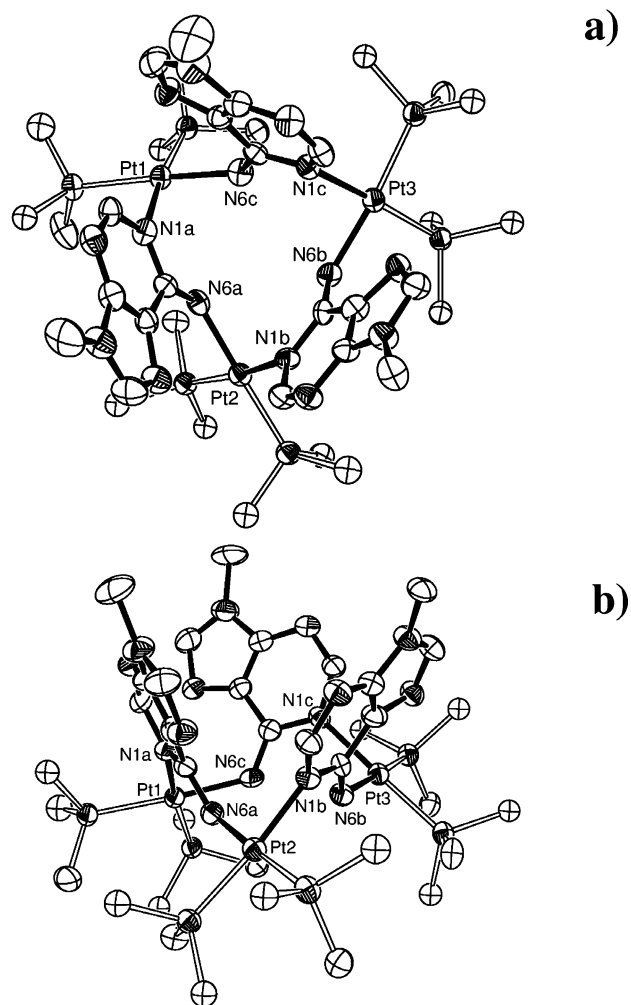


**Figure 1.** Molecular structure of one of the two crystallographically independent cations  $cis\text{-}[(\text{PMePh}_2)_2\text{Pt}\{9\text{-MeAd}(-\text{H})\}]_3^{3+}$  in **2** (phenyl rings omitted for clarity): (a) along the pseudo-3-fold axis; (b) side view.

**Table 2.** Selected Coordination Bond Lengths (Å) for **2**

1st unit		2nd unit	
Pt(1)–Pt(2)	5.204(1)	Pt(4)–Pt(5)	5.360(1)
Pt(2)–Pt(3)	5.382(1)	Pt(4)–Pt(6)	5.202(1)
Pt(1)–Pt(3)	5.320(1)	Pt(5)–Pt(6)	5.362(1)
Pt(1)–N(1a)	2.124(10)	Pt(4)–N(1d)	2.114(9)
Pt(2)–N(1b)	2.107(9)	Pt(5)–N(1e)	2.117(11)
Pt(3)–N(1c)	2.118(10)	Pt(6)–N(1f)	2.122(9)
Pt(1)–N(6c)	2.069(11)	Pt(4)–N(6f)	2.066(9)
Pt(2)–N(6a)	2.055(10)	Pt(5)–N(6d)	2.087(10)
Pt(3)–N(6b)	2.081(10)	Pt(6)–N(6e)	2.094(10)

(Table 2). The nucleobases are disposed with dihedral angle of 55–76° with respect to the metal  $\text{Pt}_3$  plane to form a pinched cone arrangement. The crystal structure evidences the two independent molecules packed head-to-head (Figure 2), in such a way that in the dimer the bases give origin to a cavity, similar to that, filled with water molecules, detected in the crystal packing of  $[\text{Pt}^{\text{IV}}\text{Me}_3\{9\text{-MeAd}(-\text{H})\}]_3 \cdot \text{OEt}_2$ .<sup>6</sup> Of the disordered water oxygen atoms detected in the crystals of **2**, none of these are inside the described voids. On the other hand, a nitrate anion is located on the phosphine side of each complex molecule, with a close approach of nitrate oxygens to Pt apical position and a short Pt–O distance of 3.26 Å being observed for Pt(2).

(10) Collaborative Computational Project, Number 4. *Acta Crystallogr., Sect. D* **1994**, *50*, 760–763.

(11) Sheldrick, G. M. *SHELX97 Programs for Crystal Structure Analysis*, release 97-2; University of Göttingen: Göttingen, Germany, 1998.

(12) Farrugia, L. J. *J. Appl. Crystallogr.* **1999**, *32*, 837–838.

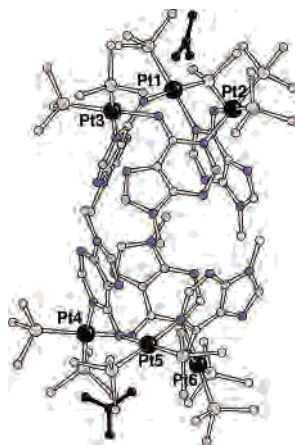


**Figure 2.** The dimer in the crystal packing of **2** showing the nitrate anions inside the area delimited by the coordination metal planes (phosphine phenyl rings and methyls not shown).

**Table 3.**  $^1\text{H}$  NMR Data ( $\delta$  in ppm) for the Adenine Complexes **2**, **3**, **5**, **6**, and **8** in  $\text{DMSO-}d_6$  and/or  $\text{CDCl}_3$  at 27 °C

compound (solvent)	H(2)	H(8)	NH <sub>2</sub> /NH	NCH <sub>3</sub>	PMe
<b>2</b> ( $\text{CDCl}_3$ ) <sup>a</sup>	7.65	8.27	7.11	3.45	1.20, 2.75
	<i>b</i>	8.14	6.82	5.80	3.70
<b>3</b> ( $\text{DMSO-}d_6$ ) <sup>c</sup>	8.04	6.52	5.25	3.56	2.12, 2.23
<b>5</b> ( $\text{DMSO-}d_6$ )	8.64	6.52	5.30	3.51	1.96, 2.25
<b>6</b> ( $\text{CDCl}_3$ )	8.01	9.94	11.08; 8.53	3.52	2.39, 2.26
					2.13, 1.96
<b>8</b> ( $\text{DMSO-}d_6$ ) <sup>d</sup>	8.95	8.12	8.6	3.60	2.32
	8.71	8.11	8.6	3.57	2.32

<sup>a</sup> First row refers to the 90% component. <sup>b</sup> Second row refers to the 10% component. <sup>c</sup> The data refer to the major component in the mixture. <sup>d</sup> First row refers to the 55% conformer.

**Table 4.**  $^{31}\text{P}$  and  $^{195}\text{Pt}$  NMR Data ( $\delta$ , in ppm;  $J$  in Hz) for the Adenine Complexes **2**, **3**, **5**, **6**, and **8** in  $\text{DMSO-}d_6$  and/or  $\text{CDCl}_3$  at 27 °C<sup>a</sup>

complex (solvent)	$\delta$ $^{31}\text{P}$	$^1J_{\text{PPt}}$	$\delta$ $^{195}\text{Pt}$
<b>2</b> ( $\text{CDCl}_3$ ) <sup>b</sup>	-8.29 (1.20, 7.11)	3150	-4217 (1.20, 2.75, 7.11)
	-9.85 (2.75, 7.65)	3360	
	<i>c</i>	-7.93 (2.35)	3750
	-8.14 (1.83)	3050	
<b>3</b> ( $\text{DMSO-}d_6$ ) <sup>d</sup>	-5.50 (2.23, 6.52)	3717	-4348 (2.12, 2.23, 5.25)
	-6.28 (2.12, 5.25)	3086	
<b>5</b> ( $\text{DMSO-}d_6$ )	-4.81 (1.96, 8.64)	3305	-4231 (1.96)
	-10.35 (1.96)	3780	
	-5.82 (2.25, 6.52)	3660	-4377 (2.25, 5.30)
	-7.15 (2.25, 5.30)	3222	
<b>6</b> ( $\text{CDCl}_3$ )	-4.13 (2.39, 8.01)	3431	-4235 (1.96, 2.39, 8.01)
	-13.74 (1.96)	3790	
	-4.76 (2.26, 9.94)	3450	-4218 (2.13, 2.26, 9.94)
	-14.78 (2.13)	3700	
<b>8</b> ( $\text{DMSO-}d_6$ ) <sup>e</sup>	-13.94 (2.32, 8.95)	3261	-4289 (2.32, 8.95)
	-13.26 (2.32, 8.71)	3249	-4281 (2.32, 8.71)

<sup>a</sup> In parentheses are reported the chemical shift values of the protons correlating with the phosphorus and platinum. <sup>b</sup> 90% component. <sup>c</sup> 10% component. <sup>d</sup> The data refer to the major component in the mixture. <sup>e</sup> First row refers to the 55% conformer.

**Stability of the Cyclic Complex *cis*-[(PMePh)<sub>2</sub>Pt{9-MeAd(-H)}<sub>3</sub>]<sup>3+</sup> (**2**) in Solution.** The  $^1\text{H}$ ,  $^{31}\text{P}$ ,  $^{195}\text{Pt}$ , and  $^{15}\text{N}$  NMR data of complex **2** are collected in Tables 3, 4, and 5, respectively, whereas  $^{13}\text{C}$  NMR data are reported in the Experimental Section. As anticipated, the NMR spectra of

**Table 5.**  $^{15}\text{N}$  NMR Data ( $\delta$  in ppm;  $J$  in Hz) for the Adenine Complexes **2**, **3**, **5**, **6**, and **8** in  $\text{DMSO-}d_6$  or  $\text{CDCl}_3$  at 27 °C

compound (solvent)	N(1)	N(3)	N(6)	N(7)	N(9)
<b>2</b> ( $\text{CDCl}_3$ ) <sup>a</sup>	-205.0	-162.0	-283.6	-132.0	-227.0
	$^2J_{\text{NP}} = 50$ Hz		$^2J_{\text{NP}} = 60$		
<b>3</b> ( $\text{DMSO-}d_6$ ) <sup>b</sup>	-132.0	-155.3	-244.7	-190.4	-217.8
			$^2J_{\text{NP}} = 50$	$^2J_{\text{NP}} = 60$	
<b>5</b> ( $\text{DMSO-}d_6$ )	-188.7	-147.2	-240.0	-188.3	-214.9
	$^2J_{\text{NP}} = 60$		$^2J_{\text{NP}} = 60$	$^2J_{\text{NP}} = 60$	
<b>6</b> ( $\text{CDCl}_3$ )	-193.8	-148.9	<i>c</i>	-198.6	-218.3
	$^2J_{\text{NP}} = 66$			$^2J_{\text{NP}} = 66$	
<b>8</b> ( $\text{DMSO-}d_6$ ) <sup>d</sup>	-200.2	-142.6	-284.0	-132.8	-218.6
	$^2J_{\text{NP}} = 60$				
	-202.8	-144.4	-284.0	-132.8	-218.6
	$^2J_{\text{NP}} = 60$				

<sup>a</sup> Data refers to the 90% component. <sup>b</sup> The data refer to the major component in the mixture. <sup>c</sup> The linewidth ( $1w_{1/2}$  70 Hz) of NH<sub>2</sub> protons, at  $\delta$  11.08 and 8.53 ppm, prevented the detection of the N(6) in inverse-detection mode. <sup>d</sup> First row refers to the 55% conformer.

**2**, obtained in chlorinated solvents, show two sets of resonances. The most intense one (ca. 90% of relative intensity) is attributable to the trinuclear species *cis*-[(PMePh)<sub>2</sub>Pt{9-MeAd(-H)}<sub>3</sub>]<sup>3+</sup>. The determination of the adenine coordination sites in this complex was achieved through appropriate two-dimensional NMR experiments. As already shown in our previous reports,<sup>3,5</sup> the first step of this process is the correct assignment of the carbons and protons of the adenine units, through  $^1\text{H}$ ,  $^{13}\text{C}$  heteronuclear multiple-quantum (HMQC)<sup>13</sup> and multiple-bond (HMBC)<sup>14</sup> correlation experiments in inverse-detection mode. The signals at  $\delta$  8.27 and 7.65 ppm were assigned to H-8 and H-2, respectively, on the basis of their different one-bond coupling constants [ $^1J(\text{C,H}) = 216$  and 208 Hz for H-8 and H-2, respectively] and of their long-range correlations with carbons at 128.3 (C-5), 154.5 (C-4), and 166.2 (C-6) ppm. Once H-2 and H-8 proton resonances were properly attributed, the sites of platination were determined from the  $^1\text{H}$ ,  $^{15}\text{N}$  inverse-detection experiments (Figure 3), which show that platination occurs at N(6) and N(1) atoms of adenine moiety. The nitrogen atoms involved in the platination process are identified by the presence of a  $^2J(\text{N,P})$  coupling constant of about 60 Hz, in the second dimension. This coupling is found for the nitrogen at -283.6 ppm [ $^1J(\text{N,H}) = 80$  Hz,  $^2J(\text{N,P}) = 60$  Hz], detected through the directly bonded NH proton at 7.11 ppm, and for the nitrogen at -205.0 ppm [ $^2J(\text{N,P}) = 50$  Hz], detected through H-2 at 7.65 ppm.

The cyclic trimer **2** is substantially stable in chlorinated solvents whereas it undergoes decomposition in DMSO or DMF. As an example, in Figure 4 is shown the  $^{31}\text{P}$  NMR spectrum of **2** obtained immediately after the sample dissolution in  $\text{CD}_2\text{Cl}_2$  (trace a) and in  $\text{DMSO-}d_6$  (trace b), respectively. Thus, the AB multiplet observed at  $\delta$  -8.30 ( $^1J_{\text{PPt}}$  3174 Hz) and -9.68 ppm ( $^1J_{\text{PPt}}$  3394 Hz) in  $\text{CD}_2\text{Cl}_2$ , attributed to the trinuclear species **2**, is completely replaced by several signals in the range  $\delta$  -2.9 to -10.6 ppm in  $\text{DMSO-}d_6$ . Among these, the AB multiplet at  $\delta$  -5.50 and -6.28 ppm, with  $^2J_{\text{PP}} = 22.1$  Hz, exhibits the highest relative

(13) Bax, A.; Griffey, R. H.; Hawkins, B. L. *J. Magn. Reson.* **1983**, *55*, 301–315.

(14) Bax, A.; Summers, M. F. *J. Am. Chem. Soc.* **1986**, *108*, 2093–2094.

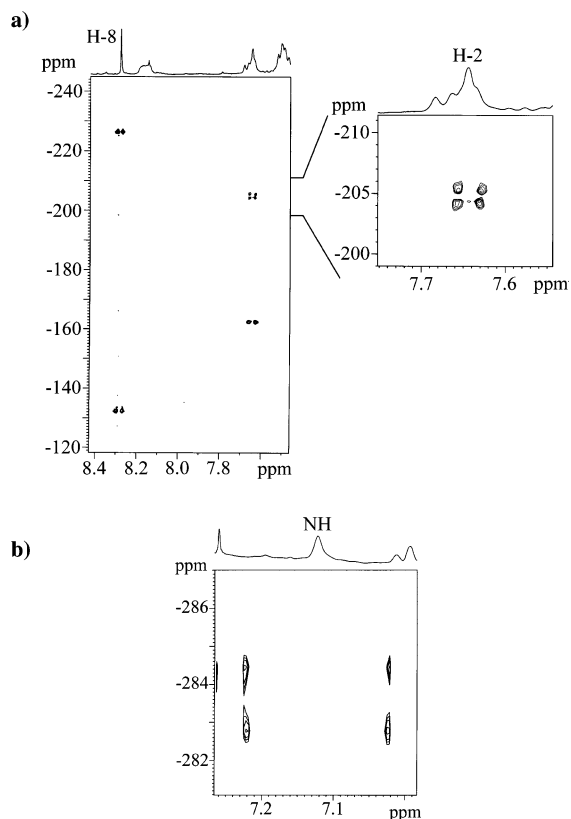


**Figure 3.**  $^1\text{H},^{15}\text{N}$  inverse-detected spectra of complex **2** in  $\text{CDCl}_3$  solution: (a) HMBC spectrum (evolution time 50 ms); (b) HMQC spectrum (5.56 ms).

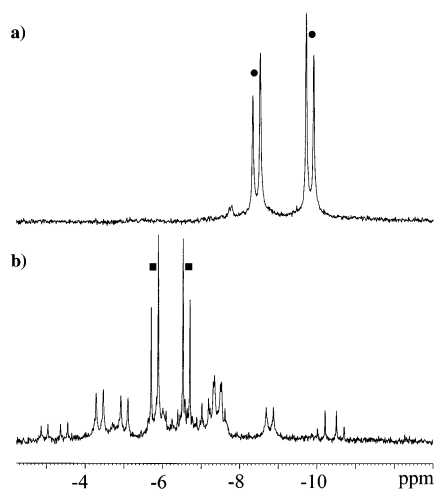


**Figure 4.**  $^{31}\text{P}\{^1\text{H}\}$  NMR spectrum (central part) of *cis*-[(PMePh<sub>2</sub>)<sub>2</sub>Pt(9-MeAd(-H))<sub>3</sub>(NO<sub>3</sub>)<sub>3</sub>], **2**, dissolved in (a)  $\text{CD}_2\text{Cl}_2$  and (b)  $\text{DMSO}-d_6$ . The label ● denotes the trinuclear species **2** whereas ■ denotes the mononuclear species **3**.

intensity. On the basis of multinuclear NMR heterocorrelated experiments, analogous to those performed on **2** in  $\text{CDCl}_3$ , we attributed this multiplet to the mononuclear species **3** containing the deprotonated N(6),N(7)-chelated nucleobase, depicted in Scheme 3. The pertinent  $^1\text{H}$ ,  $^{195}\text{Pt}$ , and  $^{15}\text{N}$  NMR data are collected in Tables 3–5.

The change in the coordination sites of the adenine moiety, induced by the variation of the solvent, is evidenced by  $^1\text{H},^{15}\text{N}$  inverse-detection experiments on **3** (Figure 5). The detected correlations, between the NH proton at 5.25 ppm

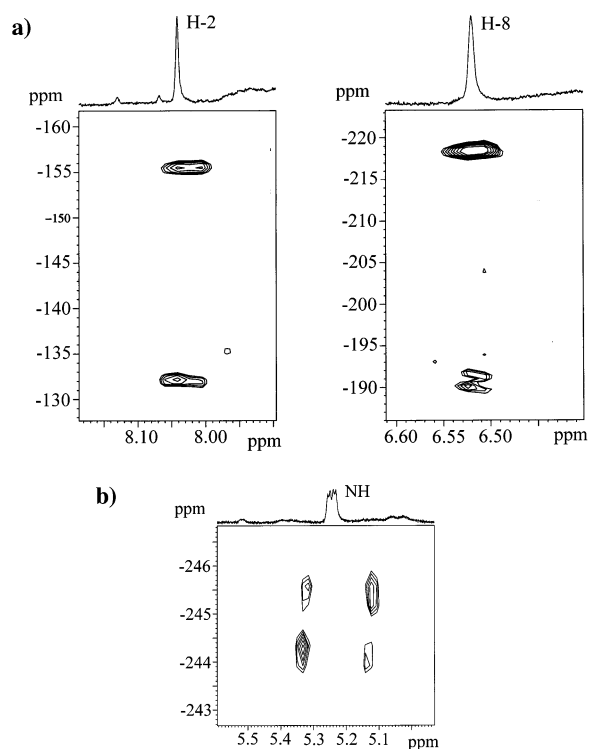
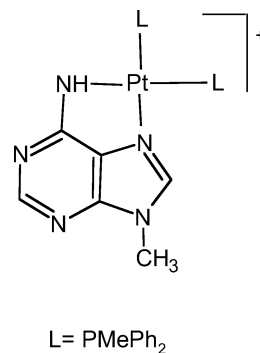


**Figure 5.**  $^1\text{H},^{15}\text{N}$  inverse-detected spectra of complex **3** in  $\text{DMSO}-d_6$  solution: (a) HMBC spectrum (evolution time 50 ms); (b) HMQC spectrum (5.56 ms).

#### Scheme 3



and the directly bonded nitrogen at  $-244.7$  ppm [ $^1J(\text{N},\text{H}) = 80$  Hz and  $^2J(\text{N},\text{P}) = 50$  Hz] and between H-8 at 6.52 ppm and the platinated nitrogen at  $-190.4$  ppm, attributable to N(7) [ $^2J(\text{N},\text{P}) = 60$  Hz], clearly indicate that the platination occurs at N(6),N(7) atoms.

We conclude that the cyclic complex **2** in DMSO is unstable and its fragmentation leads, in addition to several unknown species, to the chelated complex **3**. The formation of a chelated species is supported by  $^{195}\text{Pt}$  and  $^{31}\text{P}$  NMR data which are very similar to those obtained for the N(6),N(7) coordinated  $\text{PtL}_2$  moiety in complex **5** (see below), and this binding mode of the adenine finds precedents on Mo(IV) and Ru(II) organometallic complexes.<sup>15</sup>

The tendency of the trinuclear species **2** to rearrange, although to a minor extent, is clear also in chlorinated

(15) (a) Kuo, L. Y.; Kanatzidis, M. G.; Marks, T. J. *J. Am. Chem. Soc.* **1987**, *109*, 7207–7209. (b) Korn, S.; Sheldrick, W. S. *Inorg. Chim. Acta* **1997**, *254*, 85–91.

solvents. In fact, a very weak resonance at ca.  $\delta -8.0$  ppm is present in the  $^{31}\text{P}$  NMR of **2** in  $\text{CD}_2\text{Cl}_2$  (see Figure 4a), better characterized in  $\text{CDCl}_3$  in which is observed an AB multiplet with ca. 10% of relative intensity (see Table 4). The intensity of these signals increases upon addition of DMSO, and the chemical shift values undergo a downfield shift (in dependence on the DMSO fraction) approaching the values found for complex **3** in pure  $\text{DMSO}-d_6$ .

The disruption of **2**, which is apparently complete in DMSO (see Figure 4b), is only partial in DMF (about 20%) as estimated on the relative intensities of the signals in the  $^{31}\text{P}$  NMR spectrum. One of the products appears to be the chelated species **3** as inferred from the  $^{31}\text{P}$  parameters ( $\delta -5.58$ ,  $^1J_{\text{Pt}}$  3719 Hz, and  $-6.28$  ppm,  $^1J_{\text{Pt}}$  3045 Hz, with  $^2J_{\text{PP}} = 22.3$  Hz), very similar to those obtained in DMSO. It is important to note that the formation of **3** upon dissolution of **2** in DMF is a reversible process. In fact, complex **2** prepared in this solvent (yield 88%) exhibits NMR spectra identical to those of the product isolated from  $\text{CH}_2\text{Cl}_2$ .

**Synthesis and X-ray Structure of the Diplatinated Complex *cis*-[(PMePh<sub>2</sub>)<sub>2</sub>Pt(ONO<sub>2</sub>)<sub>2</sub>{9-MeAd(-H)}Pt(PMePh<sub>2</sub>)<sub>2</sub>](NO<sub>3</sub>)<sub>2</sub> (**5**).** We have recently reported that the analogue of complex **2** stabilized by the phosphine  $\text{PMe}_2\text{Ph}$  undergoes platination at the N(7) site of the adenine forming mainly the dinuclear species analogue of **5** depicted in Scheme 2. A similar reaction occurs when a stoichiometric amount of **2** and *cis*-[(PMePh<sub>2</sub>)<sub>2</sub>Pt(NO<sub>3</sub>)<sub>2</sub>], **4**, are mixed in DMSO or DMF, leading to the quantitative formation of the diplatinated complex **5**. The coordination of two *cis*-L<sub>2</sub>Pt units and the simultaneous involvement of N(1), N(6), and N(7) atoms of the same adenine in the platination process are indicated by NMR data obtained through heterocorrelated experiments. In particular, the  $^1\text{H}$ ,  $^{15}\text{N}$  spectrum shows that the  $^{15}\text{N}$  signal at  $\delta -188.7$  (Table 5), detected through the H-2 signal at  $\delta 8.64$  (Table 3), is attributed to the N(1) atom, whereas the resonances at  $-240.0$  [ $^1J(\text{N},\text{H}) = 80$  Hz] and  $-188.3$  ppm, detected through the NH signal at 5.30 and H-8 signal at 6.52 ppm, are attributable to the N(6) and N(7) atoms, respectively. The  $^{31}\text{P}\{^1\text{H}\}$  NMR spectrum, displayed along the  $f_1$  axis in Figure 6, shows the presence of two pairs of AB multiplets with different bandwidth, those at  $\delta -4.81$  and  $-10.35$  ppm and broader than those at  $\delta -5.82$  and  $-7.15$  ppm. These two last signals are attributed to the phosphine trans to the N(7) and N(6) atoms, respectively, on the basis of the correlations of the H-8 signal with the  $^{31}\text{P}$  signal at  $-5.82$  ppm, and of the NH resonance at 5.30 ppm with the  $^{31}\text{P}$  signal at  $-7.15$  ppm. The signal at  $\delta -4.81$  of the broader AB system shows correlation with the H-2 signal at 8.64 ppm, and is thus attributed to the phosphine trans to the N(1) adenine atom, whereas that at  $-10.35$  ppm is attributed to the phosphine trans to a solvent molecule, or to the oxygen atom of a coordinated  $\text{NO}_3^-$  group (as found in the solid state structure). The competition between the solvent and the nitrate group is probably at the origin of the high line width of these two  $^{31}\text{P}$  resonances.

For complex **5** two different  $^{195}\text{Pt}$  signals are observed in the  $^1\text{H}$ ,  $^{195}\text{Pt}$  spectrum (Table 4). It is worthwhile noting that the methyl correlations in  $^1\text{H}$ ,  $^{195}\text{Pt}$  and the  $^1\text{H}$ ,  $^{31}\text{P}$  spectra

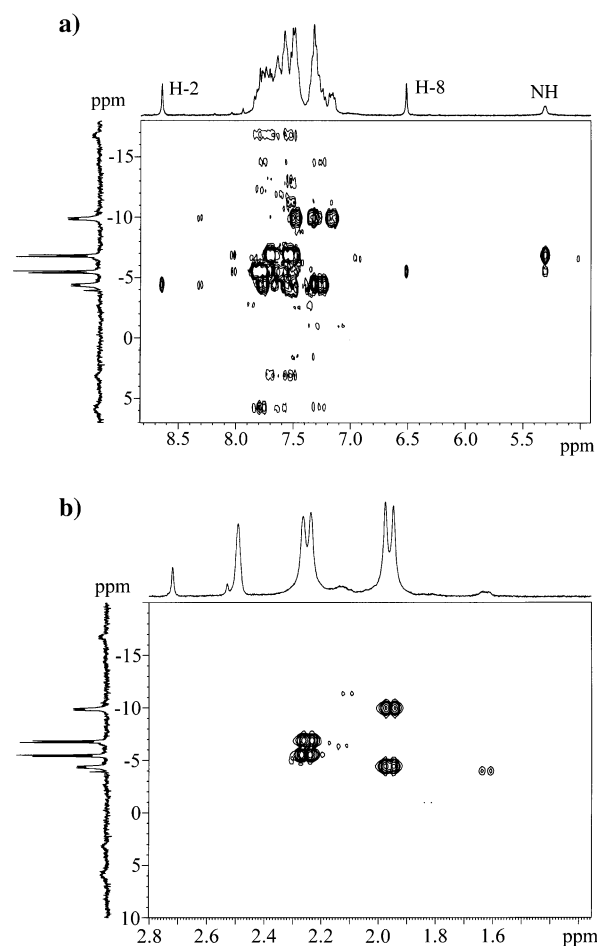


**Figure 6.**  $^1\text{H}$ ,  $^{31}\text{P}$  inverse-detected spectra of complex **5** in  $\text{DMSO}-d_6$  solution: (a) aromatic and (b) aliphatic regions.

enable the assignment of all the relevant NMR data (i.e., the methyl, phosphorus, and platinum resonances) relative to the two L<sub>2</sub>Pt moieties. Nevertheless, the unambiguous attribution of each metal center to the proper nucleobase coordination sites can be derived only through the analysis of the  $^1\text{H}$ ,  $^{31}\text{P}$  (Figure 6) and  $^1\text{H}$ ,  $^{195}\text{Pt}$  correlations (when observed) involving adenine protons.

The product obtained in DMF was isolated in good yield, and the elemental analysis of the crystals obtained from  $\text{Et}_2\text{O}$  indicates the composition  $[\text{L}_2\text{Pt}_2\{9\text{-MeAd(-H)}\}(\text{NO}_3)_2 \cdot 2\text{DMF}]$  (**5**·2DMF). The single-crystal X-ray analysis shows that one of the nitrate groups is involved in the coordination at the metal center so that the correct formula of the cationic complex is  $[\text{L}_2\text{Pt}(\text{ONO}_2)\{9\text{-MeAd(-H)}\}\text{PtL}_2]^{2+}$ . The structure of the dinuclear complex **5** is shown in Figure 7, and a selection of bond lengths and angles is reported in Table 6. The deprotonated adenine bridges the L<sub>2</sub>Pt moieties acting as monodentate to Pt(1) via N(1) and as chelating ligand to Pt(2) through N(6) and N(7) atoms. The restricted bite of the N(6), N(7) chelate induces a remarkable deviation from the ideal  $90^\circ$  angle  $\text{N(6)-Pt(2)-N(7)} = 81.3(2)^\circ$ , but both the coordination geometries, likely for steric reasons, result considerably distorted (Table 6).

The nucleobase, which is almost orthogonal to the coordination plane of Pt(1) (dihedral angle of  $83.4(1)^\circ$ ), results coplanar with that of Pt(2). Thus, the dihedral angle



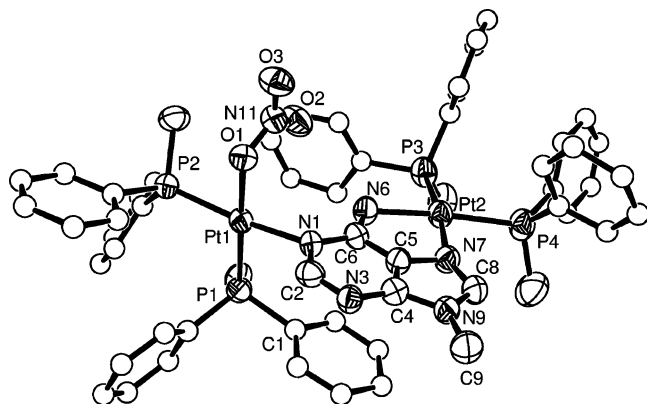


**Figure 7.** ORTEP drawing of **5** (ellipsoids at 40% probability level) with labeling scheme of relevant atoms. For clarity, carbon atoms of phenyl rings are sketched with a fixed radius.

**Table 6.** Selected Bond Lengths (Å) and Angles (deg) for **5**

Pt(1)–N(1)	2.091(6)	Pt(2)–N(6)	2.095(7)
Pt(1)–O(1)	2.109(5)	Pt(2)–N(7)	2.126(7)
Pt(1)–P(1)	2.255(2)	Pt(2)–P(3)	2.238(3)
Pt(1)–P(2)	2.278(2)	Pt(2)–P(4)	2.267(3)
N(1)–Pt(1)–O(1)	85.8(2)	N(6)–Pt(2)–N(7)	81.3(2)
N(1)–Pt(1)–P(1)	90.72(19)	N(6)–Pt(2)–P(3)	92.43(19)
O(1)–Pt(1)–P(1)	173.92(15)	N(7)–Pt(2)–P(3)	173.14(19)
N(1)–Pt(1)–P(2)	171.25(18)	N(6)–Pt(2)–P(4)	170.69(19)
O(1)–Pt(1)–P(2)	85.42(16)	N(7)–Pt(2)–P(4)	89.46(19)
P(1)–Pt(1)–P(2)	97.95(8)	P(3)–Pt(2)–P(4)	96.87(10)
C(2)–N(1)–Pt(1)	117.7(5)	C(6)–N(6)–Pt(2)	112.7(5)
C(6)–N(1)–Pt(1)	121.8(5)	C(8)–N(7)–Pt(2)	151.5(6)
N(11)–O(1)–Pt(1)	117.0(5)	C(5)–N(7)–Pt(2)	105.1(5)

is also close to the angle formed by the two metal coordination planes ( $82.2(1)^\circ$ ). Beside the phosphine groups, Pt(1) completes the square planar coordination through a nitrate oxygen at 2.109(5) Å, comparable with the values found in the dinitrate complex **4** (see below). It is worth noting in the complex cation the stacking interaction between the base and one of the phenyl rings of the P(1) phosphine which leads the ipso carbon atom to be at 3.00 Å from adenine nitrogen N(1). A similar coordination mode for the nucleobase has been reported only in two crystallographic forms of the neutral trinuclear complex  $[\text{Pt}^{\text{IV}}\text{Me}_3\{9\text{-MeAd}(-\text{H})\}]_3$ .<sup>6</sup> However, in this adduct, the Pt–N distances average to 2.20 Å for the presence of strong trans influencing methyl groups and for the geometrical requisites in the formation of the cycle, and a comparison with present data results useless.

The same coordination mode for the nitrate group found in **5** was observed in the complex **4**. The X-ray structure of **4** shows (Figure 8) the platinum bound to the P and O nitrate atoms in a distorted square planar geometry and, as expected, with a cis configuration. A selection of bond lengths and angles is reported in Table 7. The  $\text{ONO}_2$  groups are directed on opposite sides of the coordination plane, which exhibits significant tetrahedral distortions with deviations of  $\pm 0.45$  and  $\pm 0.57$  Å for nitrogen and phosphorus donors, respectively. The orientation of two phenyl rings is such to ensure a weak intramolecular  $\pi$ -interaction, the ipso carbon atoms C(9) and C(15) being at a distance of 3.50 Å (see Figure 8). The coordination bond lengths and angles and the orientation

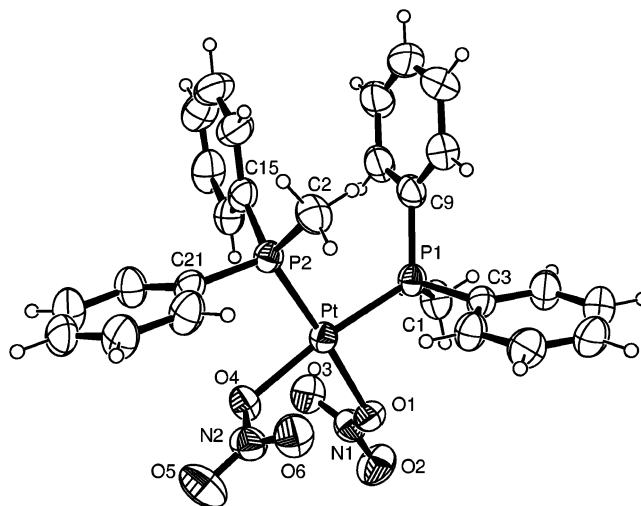


**Figure 8.** ORTEP drawing of **4** (ellipsoids at 40% probability level) with atom-labeling scheme.

**Table 7.** Selected Bond Lengths (Å) and Angles (deg) for **4**

Pt–O(1)	2.125(6)	Pt–P(1)	2.239(2)
Pt–O(4)	2.095(6)	Pt–P(2)	2.230(2)
O(4)–Pt–O(1)	84.5(3)	O(4)–Pt–P(1)	171.20(18)
P(2)–Pt–P(1)	97.07(8)	O(4)–Pt–P(2)	91.62(19)
O(1)–Pt–P(1)	86.83(18)	N(1)–O(1)–Pt	114.7(4)
O(1)–Pt–P(2)	175.44(16)	N(2)–O(4)–Pt	113.5(5)

of nitrate ions are very similar to those detected in the  $\text{PMe}_3$ <sup>16</sup> and  $\text{PET}_3$ <sup>17</sup> derivatives.

**Synthesis and NMR Studies on the N(1),N(7)-Diplatinated Complex  $cis\text{-}[\{(\text{PMePh}_2)_2\text{Pt}(\text{ONO}_2)_2\}_2(9\text{-MeAd})](\text{NO}_3)_2$  (**6**).** When 9-MeAd is added in a 1:2 molar ratio to a suspension of the nitrate complex **4** in chlorinated solvents, the complex  $cis\text{-}[\{L_2\text{Pt}(\text{ONO}_2)_2\}_2(9\text{-MeAd})](\text{NO}_3)_2$ , **6**, is formed in quantitative yield. The reaction, followed by <sup>31</sup>P NMR in  $\text{CDCl}_3$ , is complete in ca. 12 h, at ambient temperature. The multinuclear NMR characterization shows that the neutral adenine acts as a bifunctional ligand through the N(1) and N(7) atoms. The sites of platination were identified through long-range <sup>1</sup>H,<sup>15</sup>N experiments, showing that H-2 correlates with N(1) and H-8 with N(7) (see Table 5).<sup>18</sup>

The <sup>31</sup>P NMR spectrum of **6** exhibits two AX multiplets due to two pairs of coupled resonances (Table 4), as derived from a <sup>31</sup>P{<sup>1</sup>H}-homonuclear correlation experiment. The two signals at  $-4.13$  and  $-4.76$  ppm are attributed to the phosphorus atoms trans to N(1) and N(7) of adenine, on the basis of their long-range <sup>1</sup>H,<sup>31</sup>P correlations with H-2 and H-8, respectively. The resonances at  $\delta -13.74$  and  $-14.78$  ppm are assigned to the phosphines trans to the  $\text{NO}_3^-$  ligands.

The <sup>1</sup>H,<sup>195</sup>Pt correlation spectrum (Figure 9) allows us, on the basis of the correlation between H-2, H-8, and methyl

(16) Suzuki, Y.; Miyamoto, T. K.; Ichida, H. *Acta Crystallogr., Sect. C* **1993**, *49*, 1318–1320.

(17) Kuehl, C. J.; Tabellion, F. M.; Arif, A. M.; Stang, P. J. *Organometallics* **2001**, *20*, 1956–1959.

(18) The linewidth ( $l_{w/2}$  70 Hz) of  $\text{NH}_2$  protons, at  $\delta$  11.08 and 8.53 ppm, prevented the detection of the N(6) in inverse-detection mode. The large difference between these two resonances suggests the involvement of the one shifted to low-field in an intramolecular hydrogen bond, probably with a nitrate ion.

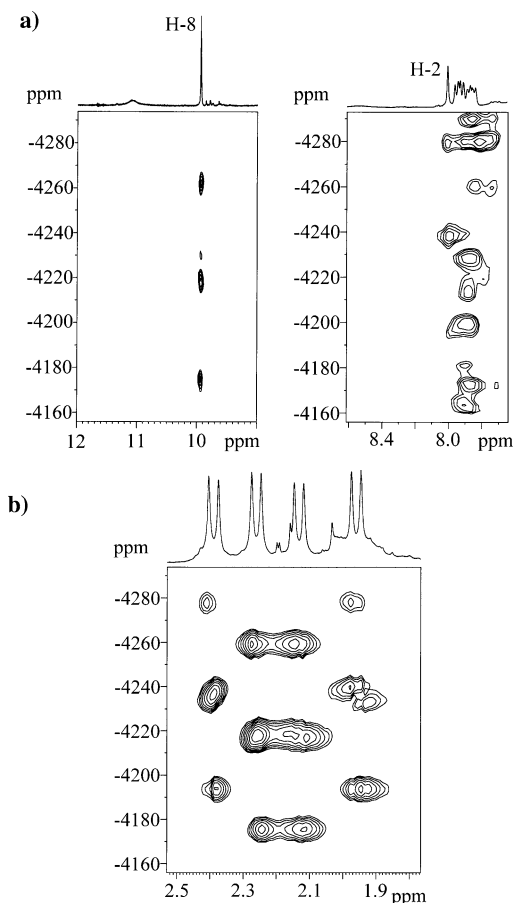


**Figure 9.**  $^1\text{H}, ^{195}\text{Pt}$  inverse-detected spectra of complex **6** in  $\text{CDCl}_3$  solution: (a) aromatic and (b) aliphatic regions. The correlation between H-2 and platinum at  $-4235$  ppm is very low and partially overlapped by correlations and  $t_1$  noise of aromatic phosphine protons.

protons with  $^{195}\text{Pt}$  signals, to establish that the signal at  $\delta -4235$  is due to the platinum bonded to N(1), whereas that at  $-4218$  ppm is due to platinum bonded to N(7). Again, this correlation experiment is fundamental for the attribution of the methyl resonances (and the related phosphines) to the proper platinum atom and for the assignment of the metal centers to the platinated nitrogens.

Pt(II) complexes containing N(1),N(7)-coordinated 9-MeAd have been structurally characterized in several cases.<sup>19</sup> We were unable to obtain crystals of **6** for the X-ray structure. As a matter of fact, a solution of **6** in  $\text{CH}_2\text{Cl}_2/\text{EtOH}$  separated crystals of the starting complex **4** (used for its X-ray analysis). The lability of **6** observed in ethanol is confirmed in DMSO. In this solvent it undergoes complete decomposition as shown in Figure 10 in which the  $^{31}\text{P}$  NMR spectra of **6**, in  $\text{CDCl}_3$  (trace a) and  $\text{DMSO}-d_6$  (trace b), are reported. In this latter solvent, the following species are identified: (a) the dinitrato complex **4**, as broad singlet at  $\delta -6.88$  (relative intensity 37%); (b) the diplatinated species **5**, as sharp AB multiplet, associated with the relatively broad AX pattern (29% of the total intensities); (c) the mononuclear adducts  $\text{cis}-[\text{L}_2\text{Pt}(9\text{-MeAd})(\text{DMSO})]^{2+}$ , **7**, and  $\text{cis}-[\text{L}_2\text{Pt}(9\text{-MeAd})_2]^{2+}$ , **8**.

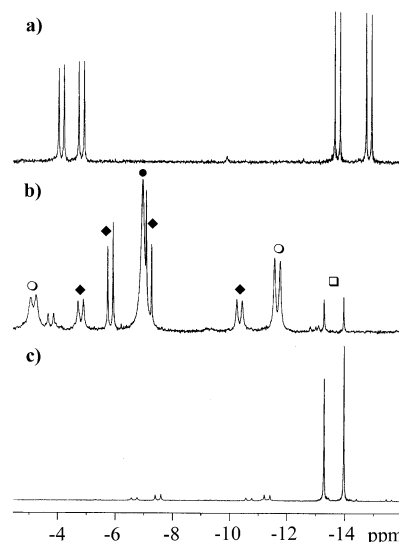


**Figure 10.**  $^{31}\text{P}\{^1\text{H}\}$  NMR spectrum (central part) of **6** in (a)  $\text{CDCl}_3$  and (b)  $\text{DMSO}-d_6$ ; (c) sample b, immediately after the addition of 9-MeAd (Pt/9-MeAd = 1:2). The labels denote the following complexes: ● (4), ◆ (5), ○ (7), and □ (8).

The last species is characterized by sharp singlets at  $\delta -13.24$  and  $-13.92$  ppm, having similar relative intensities, in agreement with the presence of two conformers, as previously shown for the  $\text{PMe}_2\text{Ph}$  and  $\text{PMe}_3$  analogues.<sup>3,5</sup> The relatively broad doublets at  $\delta -11.64$  and  $-3.13$  ppm are attributed to the monoadduct **7** (Chart 1), in which one of the ligands is a solvent molecule, whereas the doublet at  $-3.75$  ppm is unassigned. All these species were quantitatively converted into the bis-adduct  $\text{cis}-[\text{L}_2\text{Pt}(9\text{-MeAd})_2]^{2+}$  when 9-MeAd was added (9-MeAd/Pt = 2), as shown in Figure 10 (trace c).

Complex **8** was prepared by addition of 2 equiv of nucleobase to **4** in  $\text{CH}_3\text{CN}$ , characterized by elemental analysis and through multinuclear NMR spectroscopy. All NMR spectra display two major sets of resonances (Tables 3–5) attributed to the presence of two conformers at equilibrium (*head-to-head* and *head-to-tail*) in a 55:45 ratio. Also in the present case the coordination of the adenine occurs mainly ( $\geq 83\%$ , in  $\text{DMSO}-d_6$ ) at the N(1) atom, as evidenced by  $^1\text{H}, ^{15}\text{N}$  heteronuclear correlation experiments. The minor resonances in the  $^{31}\text{P}$  NMR spectrum of Figure 10c can be likely attributed to the coordination isomer  $\text{cis}-[\text{L}_2\text{Pt}(9\text{-MeAd}-N')(9\text{-MeAd}-N'')]^{2+}$ , in which one of the two adenine molecules is N(7)-coordinated.

## Conclusions

The results reported in this paper can be summarized as follows: (i) The deprotonation of the adenine at the  $\text{NH}_2$  group induced by the hydroxo complex  $\text{cis}-[\text{L}_2\text{Pt}(\mu\text{-OH})]_2^{2+}$  affords the species  $\text{cis}-[\text{L}_2\text{Pt}\{9\text{-MeAd}(-\text{H})\}]_3^{3+}$  ( $\text{L} = \text{PMePh}_2$ , **2**), which represents the first example of a cyclic trimer of the nucleobase N(1),N(6)-platinated structurally characterized. (ii) Unlike its  $\text{PMe}_2\text{Ph}$  analogue,<sup>5</sup> complex **2** in coordinating solvents undergoes solvolysis, and one of the reaction products is the mononuclear species **3**, in which the adenine is N(6),N(7)-chelated. (iii) The trinuclear complex **2** can be quantitatively converted into the dinuclear species

(19) (a) Lock, C. J. L.; Speranzini, R. A.; Turner, G.; Powell, J. J. *Am. Chem. Soc.* **1976**, *98*, 7865–7866. (b) Jaworski, S.; Menzer, S.; Lippert, B.; Sabat, M. *Inorg. Chim. Acta* **1993**, *205*, 31–34.

**5** in which the adenine exhibits a new binding mode, previously characterized in solution for the  $\text{PMe}_2\text{Ph}$  derivative. (iv) The NMR study of complex **6** in DMSO gives a clear evidence that the simultaneous presence of two *cis*- $\text{L}_2\text{Pt}$  units at the N(1),N(7) sites of the adenine promotes the reversible deprotonation of the exocyclic amino group. As expected, the addition of the strong base 1,8-bis-(dimethylamino)naphthalene (“proton sponge”) to the solution of **6** leads to the quantitative formation of the deprotonated species **5**. (v) The information derived from the multinuclear NMR analysis is essential for the structural characterization in solution of these platinum–adenine complexes stabilized by phosphine with phenyl groups. It is apparent that the chemical shift of the adenine protons H-2, H-8, and NH cannot be directly used for the assignment of

the platination sites. The position of these signals, in fact, is largely variable (especially for H-8), likely as the result of anisotropy effects due to the presence of aromatic rings on the phosphine ligands.

**Acknowledgment.** Thanks are due to the Centro Interdipartimentale Grandi Strumenti of Modena University for the use of the Bruker AMX 400 WB spectrometer. This work was financially supported by the Ministero dell’Università e della Ricerca Scientifica e Tecnologica, PRIN 2001.

**Supporting Information Available:** Crystallographic data for the structures reported in this paper. This material is available free of charge via the Internet at <http://pubs.acs.org>.

IC034406Z